19th IMEKO TC10 Conference
"MACRO meets NANO in Measurement for Diagnostics, Optimization and Control"
Delft, The Netherlands, September 21–22, 2023

Detection of Broken Bar Fault in Induction Motor Using Higher-Order Harmonics Analysis

Alexander Shestakov, Dmitry Galyshev, Victoria Eremeeva, Vladimir Sinitsin, Olga Ibryaeva

South Ural State University, Chelyabinsk, Russia, ibriaevaol@susu.ru

Abstract – The induction motors are a part of the bulk critical actuators in metallurgy, engineering and other industries. Generally, industries technological processes limit a redundancy of the critical actuators. Therefore, condition monitoring of the critical actuators parts is the basis of efficiency and reliability of the processes. In turn, the special operate conditions of the actuators, like unsteady speed and load, affects the motor condition monitoring success significantly. Induction motor rotor defects such as squirrel cage damage are minor but leads to unpredicted shutdown and greater maintenance costs. The present study presents a reliable method for detecting defects in squirrel cage rotor bars of the actuator induction motor which runs at various speed and load. The method is based on higher-order space harmonics processing in the motor current signal. The method combines normalization, filtering by variational mode decomposition, wavelet transform and train a convolutional neural network. The method generates a diagnostic model which allows to diagnosis motor rotor bar fault at various speed and load. At the same time, the model requires only one frequency and load for training. The experimental results show the model, which is trained at 35 Hz rotary speed, detects a rotor bar fault at 15 to 50 Hz rotary speed and up to 36% load of the nominal torque with 97% average accuracy. The proposed method is effective for the real equipment operating conditions which have limits of completeness datasets acquisition for training.

Keywords – Induction Motor, Broken Bar, Diagnostic, Current Signal Analysis, Variational Mode Decomposition, Scalogram, Convolutional Neural Network

I. INTRODUCTION

A broken bar of a squirrel-cage rotor of an induction motor is up to 10% of all faults [1]. Breakage of the rotor bar leads to an increase in power consumption and a drop in the operating torque of the motor [2]. In addition, the broken bar can lead to secondary failures such as the increase in vibration caused by the defect leads to rapid wear of the rotor support bearings. Also, broken bar can lead to rotor jamming and stator winding damage during motor operation. Therefore, the rotor bar fault detection is very important task.

The existing diagnostic methods are based on the detection of the spectral harmonic of a defect, equal to $f_{BB} = 2s * f_s$, where f_s is the supply frequency, s is the motor slip. The harmonic creates sidebands in an amplitude spectrum of the current signal [3] is defined as

$$f_{Sidebands} = (1 \pm 2s)f_s. \quad (1)$$

The sidebands are proven signs of a defect, but in some cases they are unreliable. The load on the motor shaft is a prerequisite for the sideband harmonics detection. In addition, some operating conditions lead to masking of the sideband harmonics [4]. Thus, cyclic loading, magnetic asymmetry and axial air ducts generate harmonics in the same frequency range as the 'broken bar' harmonics in the current signal. As a result, the diagnostic procedure can lead to spurious results and financial loss due to unnecessary maintenance work.

Some researchers propose an analysis of transient currents during motor start-up [5] in order to bypass the problem. The evolution of the harmonic f_{BB} is clearly visible in the current signal in the start mode due to the change in slip s from 1 to 0. At the same time the evolution differs from the effects of cyclic loading which leads to the defect and masking effects are effectively separated. However, the authors note that approach is not suitable to motors powered by inverter converters. The motor slip keeps low over the start when powered by the inverter. As result, the defects are invisible. In addition, the approach is not recommended for medium and large motors [6].

Along with traditional sidebands (1) higher-order harmonics contain information about rotor bars condition. The rotor bar fault leads to arise space harmonics about 5th and 7th harmonics of the current supply frequency [7] (Fig. 1). The space harmonics are caused by the magnetomotive force and rotation relative to the rotor and stator. The space harmonics are defined as [7]:

$$f_{Space\ harmonic} = (k(1-s) \pm s)f_s, \quad (2)$$

$$f_{Time\ harmonic} = (k \pm 2ns)f_s, \quad (3)$$

where $k = 5, 7,\ n = 1, 2, 3 \ldots$

The higher-order harmonics contain load-related harmonics as well. But the load-related harmonics produce less masking effect than around supply frequency. Thus, the frequency spectrum analysis of the current signal around the 5th and 7th harmonics of the supply frequency is a more reliable diagnostic approach.

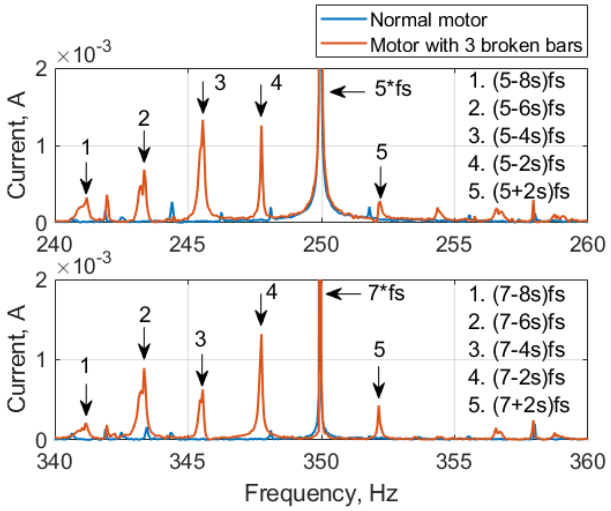

Fig. 1. Harmonics of the defect in the region 5th and 7th harmonics of the supply frequency fs=50 Hz

The present paper proposes a diagnostic method of induction motor broken rotor bar which is based on the current signal higher-space harmonics analyze. In the proposed method, current signals with different motor supply frequencies are normalized relative to each other. Then, each signal is subjected to mode decomposition using the Variational Mode Decomposition (VMD). Mode decomposition is necessary to isolate useful signal components near the 7th harmonic of the supply frequency. After, the rest of the signal is converted into a set of images in the form of scalograms by wavelet-transform. A test set of images for one supply frequency value is used to train a convolutional neural network (CNN). Then, the performance of the neural network is evaluated on data for other supply frequencies.

The work is organized as follows. Section 2 describes the proposed diagnostic method. The description of the experiments and the results of testing the proposed diagnostic method on signals are presented in Section 3. We consider two cases of the problem of induction motor fault diagnosis with variable-frequency drive (VFD) control 1) under different supply frequencies, loads and scalar V/f control and 2) under constant load and vector control. For VFD-fed induction motor's operation, the changing frequency at the VFD output might affect or even invalid an induction motor fault diagnosis approach that is functional at a fixed operating frequency [8]. We use the matrix pencil method [9] to find the variable supply frequency to adapt our method to this case.

The main contribution of the paper is the higher-order space harmonics can be considered as a diagnostic criterion in detecting broken rotor bars. The method is tested on real signals and its effectiveness is presented.

II. THE METHOD PROPOSED

Figure 2 shows the flowchart of the proposed method. It works with motor current signals at different shaft speeds. Variable rotation speed is provided by supplying voltage of different frequency from the inverter converter. Therefore, current signals at different speeds have different sine frequencies.

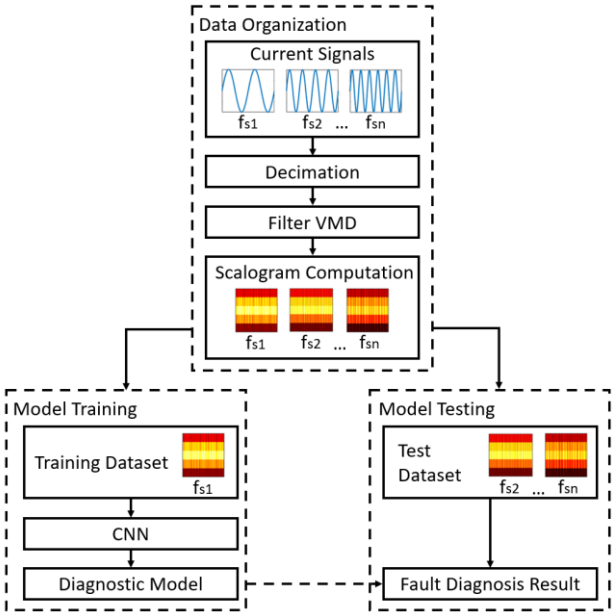

Fig. 2. Flowchart of the method

First of all, it is necessary to normalize signals with different supply frequencies relative to each other. To do this, each signal is subjected to decimation. The new sampling rate is chosen to be $F_{sample} = 20 * f_s$.

A preliminary analysis of the Fourier amplitude spectrum of the current signal with a defect showed that the signs of a defect are most pronounced in the region of the 7th supply harmonic. As a filtering, the signal is decomposed into IMF (Intrinsic Mode Functions) modes using VMD (Variational Mode Decomposition) [10]. Each IMF mode has only one central frequency. VMD identifies the important center frequencies directly from the data, but we can specify them ourselves, which is what we did.

VMD decomposition of the current signal into components with frequencies $f_s, 3f_s, 5f_s, 7f_s, 7f_s$, where f_s is the supply frequency, is presented in Fig. 3.

For further analysis, a mode containing signal components in the region of the 7th supply harmonic is selected.

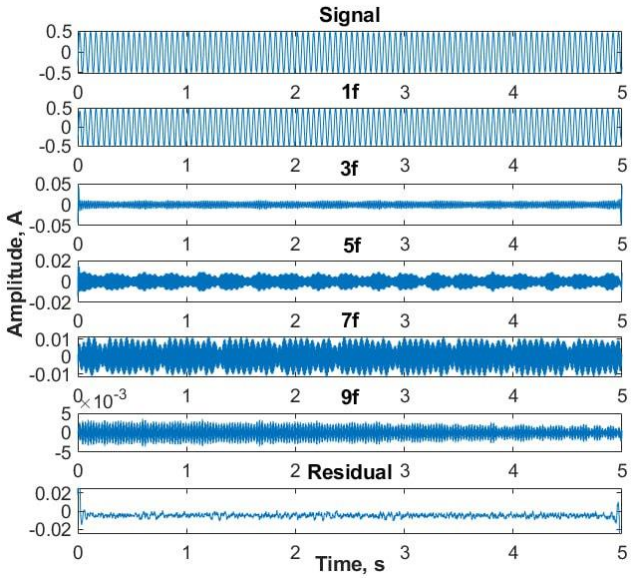

Fig. 3. VMD of the current signal

Next, the received signal is divided into the fragments. The defect harmonic f_{BB} does not depend on the supply frequency, but depends on the motor load. Therefore, the harmonic of the defect will vary within some small limits (1-2 Hz). In order for each fragment of the signal to have the same number of defect harmonic periods, the length of the fragment is chosen equal to $L = 50 * f_s$. Thus, each fragment will fit the following number of periods:

$$N = \frac{L}{F_{sample}} * f_{BB} = \frac{50f_s}{20f_s} * f_{BB} = 2{,}5f_{BB}. \quad (4)$$

The received signal fragments are converted into a scalograms for the wavelet decomposition coefficients. The frequency range is from $6f_s$ to $8f_s$. Figs. 4, 5 present scalograms for different load level. It can be seen that the images with a bar defect have a characteristic periodic pattern.

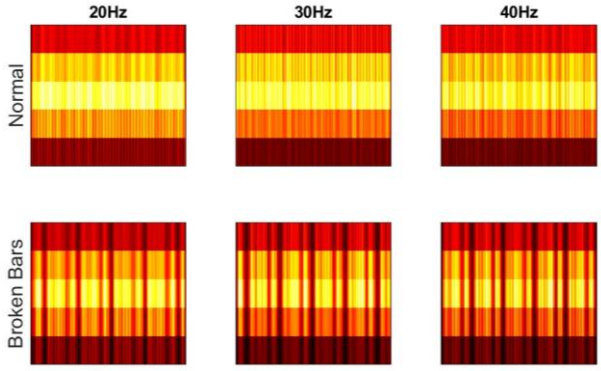

Fig. 4. Scalograms of signal fragments (low load)

The images are converted to monochrome and fed to the input of a CNN (Fig. 6).

A trail-and-error analysis was carried out to determine the CNN model parameters. The first convolutional layer contained 32 convolution kernels and outputted 32 feature maps with a size of 127×127 (we used zero padding to have the same size of output feature-maps). The MaxPooling layer (2 ×2) outputted 32 pooling maps with a size of 63×63. The second convolutional layer produced 64 feature maps with a size of 63×63 and the next pooling layer provided 64 pooling maps with a size of 31×31. After the third convolutional layer, we have 128 maps with a size of 31×31 which than flatten in a layer with 4096 neurons. An output from the flatten level is passed to two Dense layers and output layer.

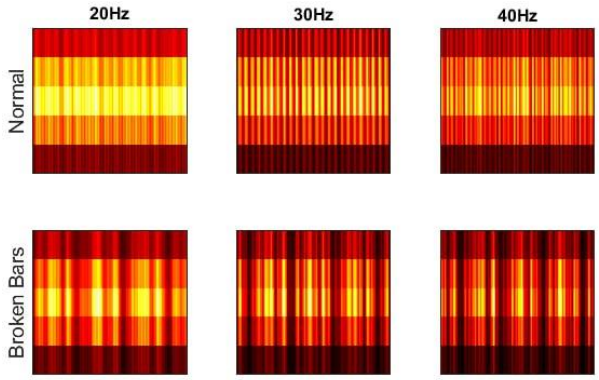

Fig. 5. Scalograms of signal fragments (medium load)

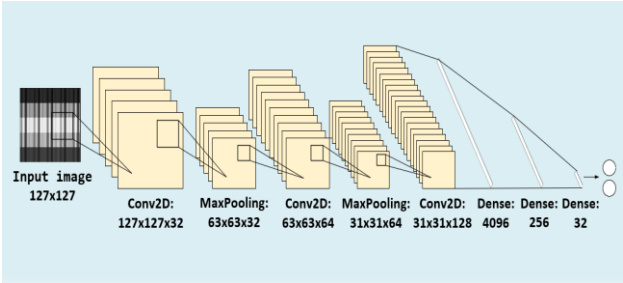

Fig. 6. Convolutional neural network model

III. RESULTS AND DISCUSSIONS

A. Case study 1. Induction motor under scalar V/f control, variable supply frequency and load

The experimental rig (Fig. 7) contains a set of induction motor with health and fault conditions. The motor works with VFD in scalar mode. The motor with fault condition contains a rotor with drilled holes in the area of the bars. All parameters of motor are shown in the Table 1.

The current clamp was placed on the phase conductor to measure the current signal of one phase. The signals were sequentially taken at different supply frequencies. The supply frequency varied from 15 Hz to 50 Hz in 5 Hz increments. Also, the signals were taken at three levels of load on the motor shaft: M1 = 2%, M3 = 20%, M5 = 36% of the nominal torque. There are 24 signals in total. The sampling rate was 50 kHz. The duration of the signal was 60 seconds.

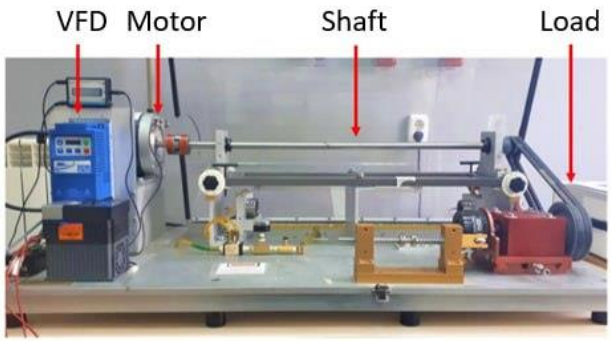

Fig. 7. Experimental rig 1

Table 1. Parameters of the motor

Nominal power, kW	0,37
Nominal voltage, V	220
Nominal frequency, Hz	50
Nominal torque, N*m	1.24
Number of all bars of rotor	34
Number of broken bars	3

Examples of signal spectra in the region of the 7th supply harmonic are shown in Figure 8. As can be seen, defect harmonics are present in the spectrum regardless of the load and supply frequency. The images of the seventh harmonic spectrum are very similar to each other, which gives the prospect of obtaining a good defect recognition model based on the analysis of this particular signal component.

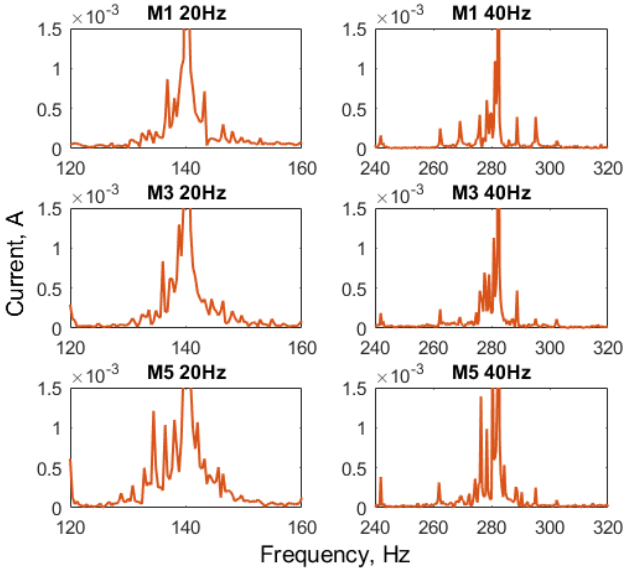

Fig. 8. Examples of signal spectra

The test data set contained scalograms of current signals with different supply frequencies and different motor loads. Due to the limitations of the initial data set, images were composed of intersecting fragments with the addition of a small step.

The CNN model (Fig. 6) was trained on a set of images for a supply frequency of 35 Hz at the M3 load. The training lasted 150 epochs. The learning curves are shown in Fig. 9.

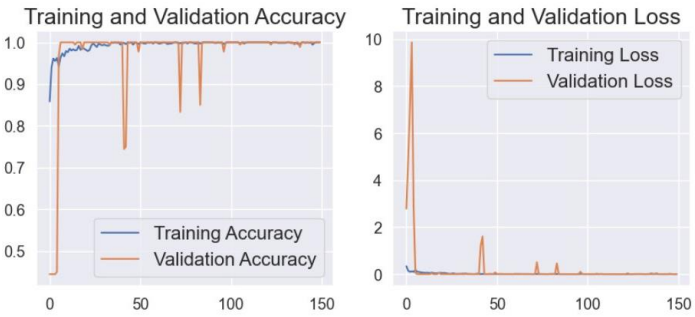

Fig. 9. Learning curves

The trained model was tested on all other sets of images. The obtained accuracy values are shown in the Fig. 10.

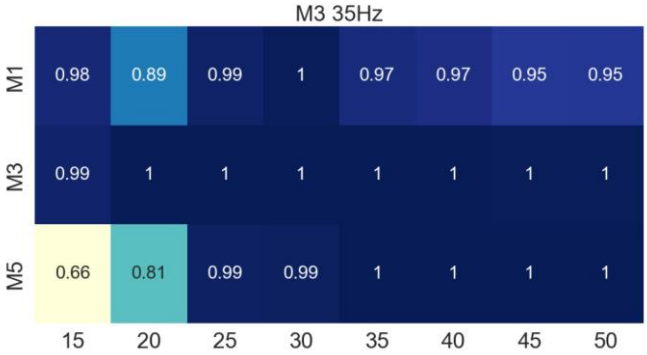

Fig. 10. Accuracy matrix for all datasets for the model trained on 35 Hz and M3 load

The model gives the best accuracy values on datasets with load and supply current values close to those on which it was trained. Data with M1 load is difficult for the classification, as well as with the lowest frequency of 15 Hz at M5 load. The average accuracy of the model was 97%, the minimum accuracy was 66 %.

Figure 11 shows a similar result for the model trained on data with a supply frequency of 35 Hz and M5 load.

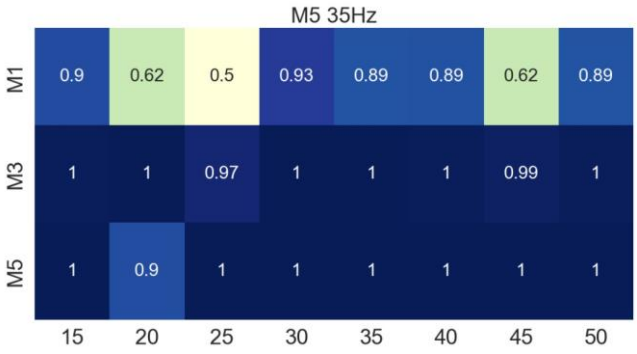

Fig. 11. Accuracy matrix for all datasets for the model trained on 35 Hz and M5 load

The model gives almost perfect accuracy on datasets with a load of M3 and M5, however, the accuracy on datasets with a load of M1 has dropped significantly compared to the old result.

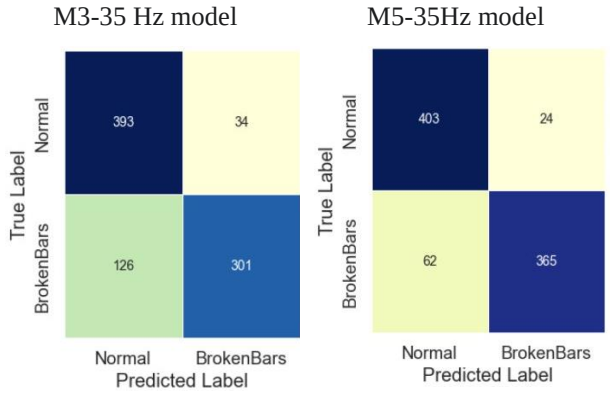

Fig. 12. Confusion matrices for the dataset with the supply frequency 20 Hz and M5 load

It can be seen that the second model gives a better accuracy value than the first model (0.9 instead of 0.81) on a dataset with a supply frequency of 20 Hz and a load of M5. The confusion matrices in Fig. 12 show that the quality of recognition of defective samples has grown significantly.

As we see, in the case of changing conditions, the model works well with similar data. If the load and/or supply frequency differ significantly, the model is more likely to be wrong.

B. *Case study 2. Induction motor under vector control, variable supply frequency and pump load*

In this Section, the proposed method is used for current data for the induction motor fed by VFD in vector mode, subjected to healthy and faulty cases under a pump load.

The experimental rig is presented in Fig. 13.

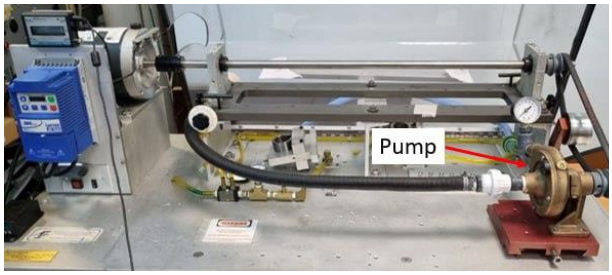

Fig. 13. Experimental rig 2

An Oberdorfer 60P centrifugal pump is installed on an experimental stand as a load for the induction motor. The pump is connected to the motor via a belt drive. The pump rotation speed matches the motor speed. The frequency converter controls the motor in vector mode while maintaining a constant output torque. The power frequency varied from 15 to 35 Hz in 10 Hz increments. The sampling rate was 70 kHz. The duration of the signal was 90 seconds.

The distinctive feature of this experiment is the variable supply frequency caused by the variable frequency drive control. Fig. 14 represents a fragment of the current signal taken from the motor with broken bars. Even though it looks like a pure sine wave, its supply frequency changes over time. Fig.15 shows the change in frequency of 7th supply harmonic over 20 seconds.

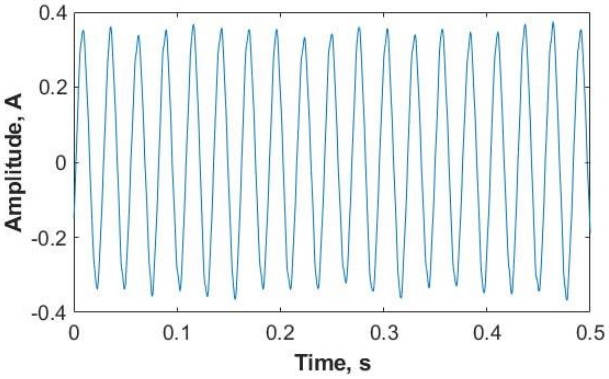

Fig. 14. Current signal

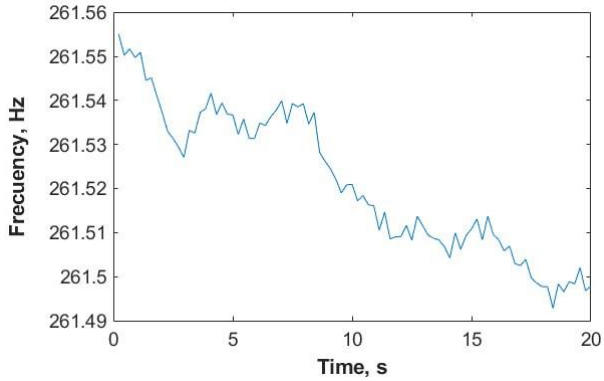

Fig. 15. Frequency of 7th supply harmonic

We use the Matrix Pencil Method (MPM) [9] to find the frequency. MPM allows us to estimate signal parameters $y(t) = \sum_{k=1}^{M} R_k e^{(\alpha_k + i\omega_k)t}$ from its samples $y(nT) = \sum_{k=1}^{M} R_k e^{(\alpha_k + i\omega_k)nT} = \sum_{k=1}^{M} R_k z_k^n$, where T is the sampling period, $R_k = A_k e^{i\varphi_k}$ are the complex amplitudes, α_k are the damping factors, $\omega_k = 2\pi f_k$ are the frequencies and $z_k = e^{(\alpha_k + i\omega_k)T}$ are the poles of $y(t)$. MPM finds the poles z_k as the solution of a generalized eigenvalues problem by using the matrix pencil formed from the sampled values $y(nT) = y_n$, $n = 0,1, \dots, N-1$, Knowing z_k we can find f_k.

Fig. 16 shows the confusion matrices for the cases of two different training datasets. In the first case we use current signals with a supply frequency of (approximately) 25 Hz. Testing the trained model on data with three different frequencies of 15, 25, 35 Hz gives accuracies of 0.91, 0.99, 0.98. The confusion matrices can be seen in the first column of Fig. 16. In the second case, training is carried out on data with a frequency of 35 Hz and the

corresponding accuracies for data with frequencies of 15, 25, 35 Hz are 0.87, 0.93, 1.

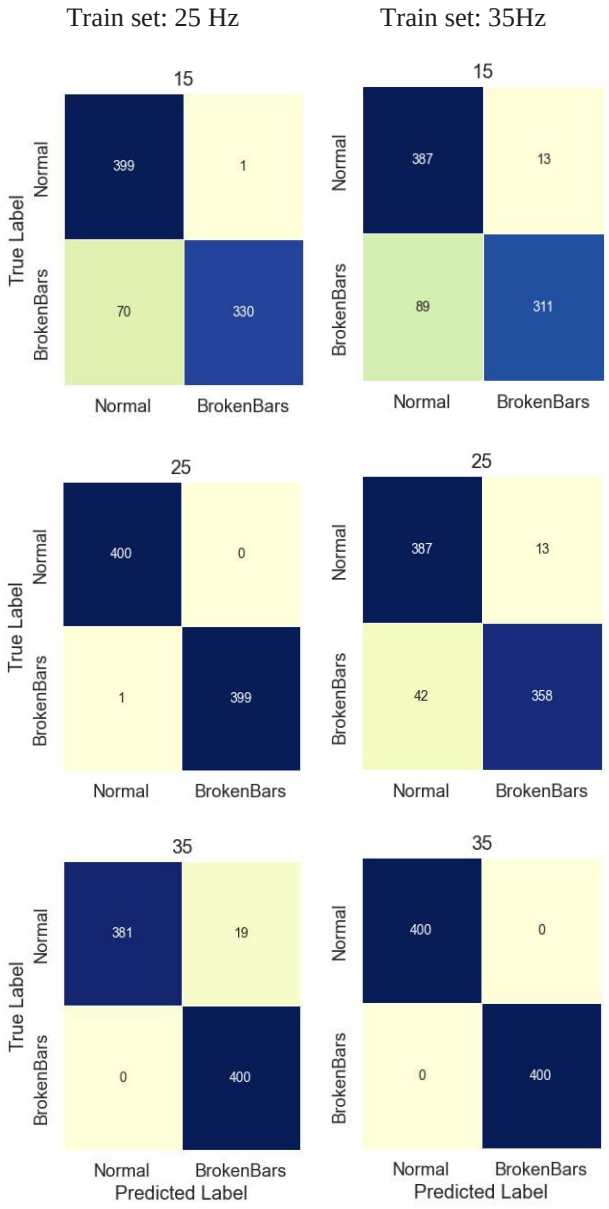

Fig. 16. Confusion matrices for different training sets

As in the previous example, we see that the trained model works better on similar data. When we changed the training set frequency from 25 to 35 Hz, the 15 Hz data was classified worse.

IV. CONCLUSIONS AND OUTLOOK

In this article, we have described a method for diagnosing broken rotor bars using the higher-order space harmonics of the current signal. As it was shown (Fig.10), the model trained at one supply frequency with one load level also works for other supply frequencies with another load values. The maximum accuracy is 100%, the average accuracy is 97%. The method can be transferred to the case of variable frequency drive and variable supply frequency.

Thus, the method performed well in conditions where training data is limited (in the examples considered, the training set consisted of only 1000 images) and when the supply frequency is variable. This can be very useful in real production environments where we usually deal with VFD-fed induction motor it is not always possible to collect a lot of defective data. Further work will be directed to the study of other types of faults.

V. ACKNOWLEDGMENTS

This work was financially supported by Ministry of Science and Higher Education of the Russian Federation (FENU-2023-0010).

REFERENCES

[1] **Singh, G.K., Sa'ad Ahmed Saleh Al Kazzaz:** Induction machine drive condition monitoring and diagnostic research – a survey, *Electric Power Systems Research*, Vol. 64., No. 2., 2003., pp. 145-158.

[2] **Garcia, M., Panagiotou, A., et al.:** Efficiency Assessment of Induction Motors Operating Under Different Faulty Conditions, *IEEE Transactions on Industrial Electronics*, Vol. 66., No. 10., 2019, pp. 8072-8081.

[3] **Lee, S.B., Stone, G.C., Antonino-Daviu, J., Gyftakis, K.N., Strangas, E.G., Maussion, P., Platero, C.A.:** Condition monitoring of industrial electric machines: state of the art and future challenges, *IEEE Industrial Electronics Magazine*, Vol. 12., 2020, pp. 158-167.

[4] **Lee, S.B, Hyun, D., Kang, T., Yang, C., Shin, S., Kim, H., Park, S., Kong, T., Kim, H.:** Identification of false rotor fault indications produced by online MCSA for medium-voltage induction machines, *IEEE Transactions on Industry Applications*, Vol. 52., No. 1., 2016, pp. 729-739.

[5] **Antonino-Daviu, J.A., Riera-Guasp, M., Folch, J.R., Palomares. M.P.M.:** Validation of a new method for the diagnosis of rotor bar failures via wavelet transform in industrial induction machines, *IEEE Transactions on Industry Applications*, Vol. 42., No. 4., 2006, pp. 990-996.

[6] **Zhang, P., Du, Y., Habetler, T.G., Lu B.:** A Survey of Condition Monitoring and Protection Methods for Medium-Voltage Induction Motors, *IEEE Transactions on Industry Applications*, Vol. 47., No. 1., 2011, pp. 34-46.

[7] **Tang, J., Yang, Y., Chen, J., Qiu, R., Liu, Z.:** Characteristics Analysis and Measurement of Inverter-Fed Induction Motors for Stator and Rotor Fault Detection, *Energies*, Vol. 13., No. 1., 2020, p. 101.

[8] **Zaman, S., Liang, X., Li, W.:** Fault Diagnosis for Variable Frequency Drive-Fed Induction Motors Using Wavelet Packet Decomposition and Greedy-Gradient Max-Cut Learning, *IEEE Access*, Vol. 9, 2021.

[9] **Hua Y., Sarkar T. K.:** Matrix Pencil Method for Estimating Parameters of Exponentially Damped / Undamped Sinusoids in Noise, *IEEE Trans. Acoust.*, vol. 38, no. 5, 1990, pp. 814–824.

[10] **Dragomiretskiy, K., Zosso, D.:** Variational Mode Decomposition, *IEEE Transactions on Signal Processing*, 62, 2014, pp. 531-544.